

Supplementary Information: Impact of Iodide Ions on the Speciation of Radiolytic Transients in Molten LiCl-KCl Eutectic Salt Mixtures

Jacy K. Conrad,^{a*} Kazuhiro Iwamatsu,^b Michael E. Woods,^c Ruchi Gakhar,^c Bobby Layne,^b Andrew R. Cook,^b and Gregory P. Horne^{a*}

^a *Center for Radiation Chemistry Research, Idaho National Laboratory, Idaho Falls, ID, P.O. Box 1625, 83415, USA.*

^b *Department of Chemistry, Brookhaven National Laboratory, Upton, New York, 11973, USA.*

^c *Advanced Technology of Molten Salts, Idaho National Laboratory, Idaho Falls, ID, P.O. Box 1625, 83415, USA.*

*Corresponding authors. E-mail: jacy.conrad@inl.gov and gregory.horne@inl.gov.

ORCID

Jacy K. Conrad	0000-0002-0745-588X
Kazuhiro Iwamatsu	0000-0002-5977-6896
Michael E. Woods	0000-0001-8685-6026
Ruchi Gakhar	0000-0002-7103-1256
Bobby Layne	0000-0002-1225-3596
Andrew R. Cook	0000-0001-6633-3447
Gregory P. Horne	0000-0003-0596-0660

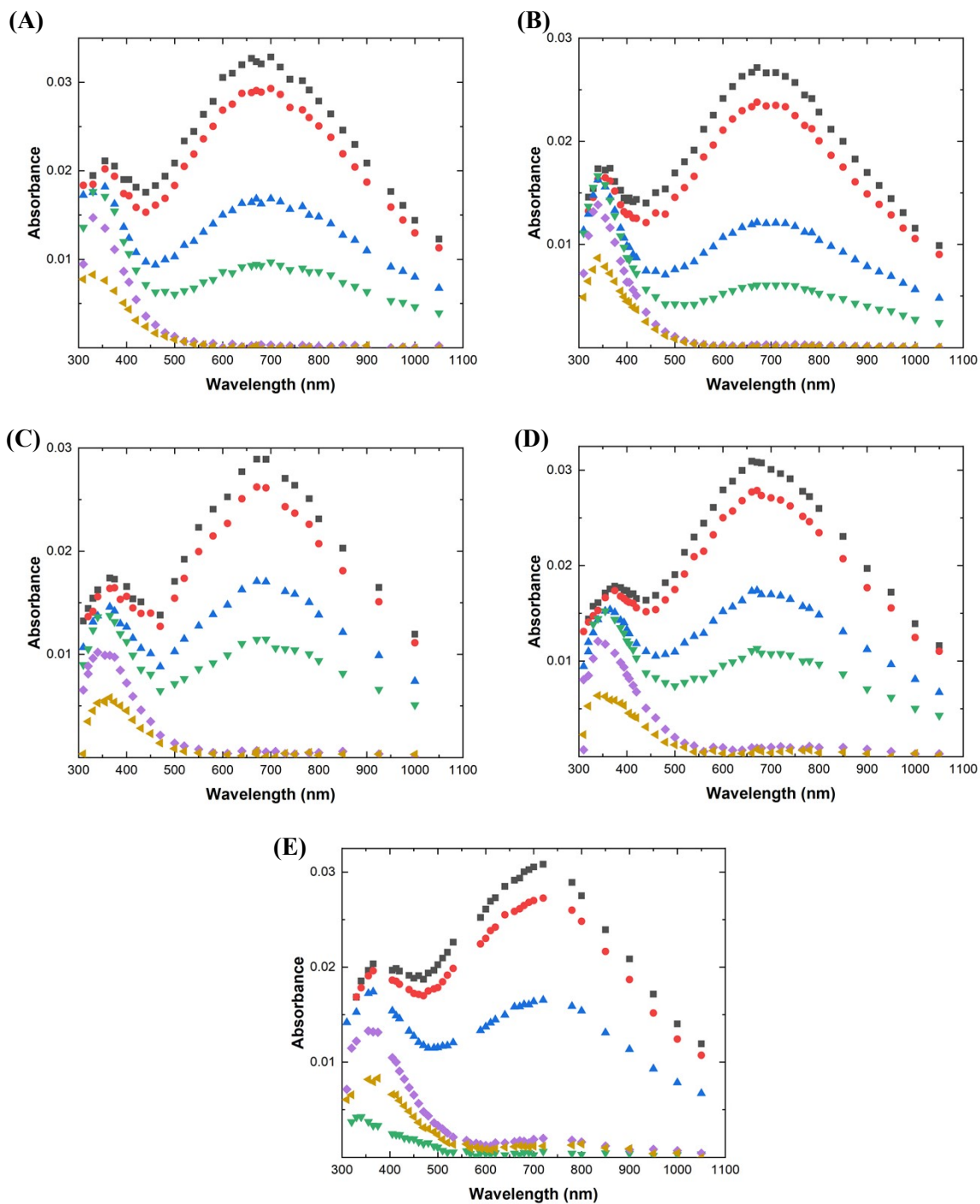


Fig. S1. Transient absorption spectra from the electron pulse irradiation of 0.054 (A), 0.107 (B), 0.536 (C), 1.072 (D), and 5.107 (E) wt.% KI in LiCl-KCl eutectic at 400 °C for 5 ns (■), 10 ns (●), 50 ns (□), 100 ns (▼), 1 μs (◆), and 5 μs (◇) normalized by the absorbed dose.

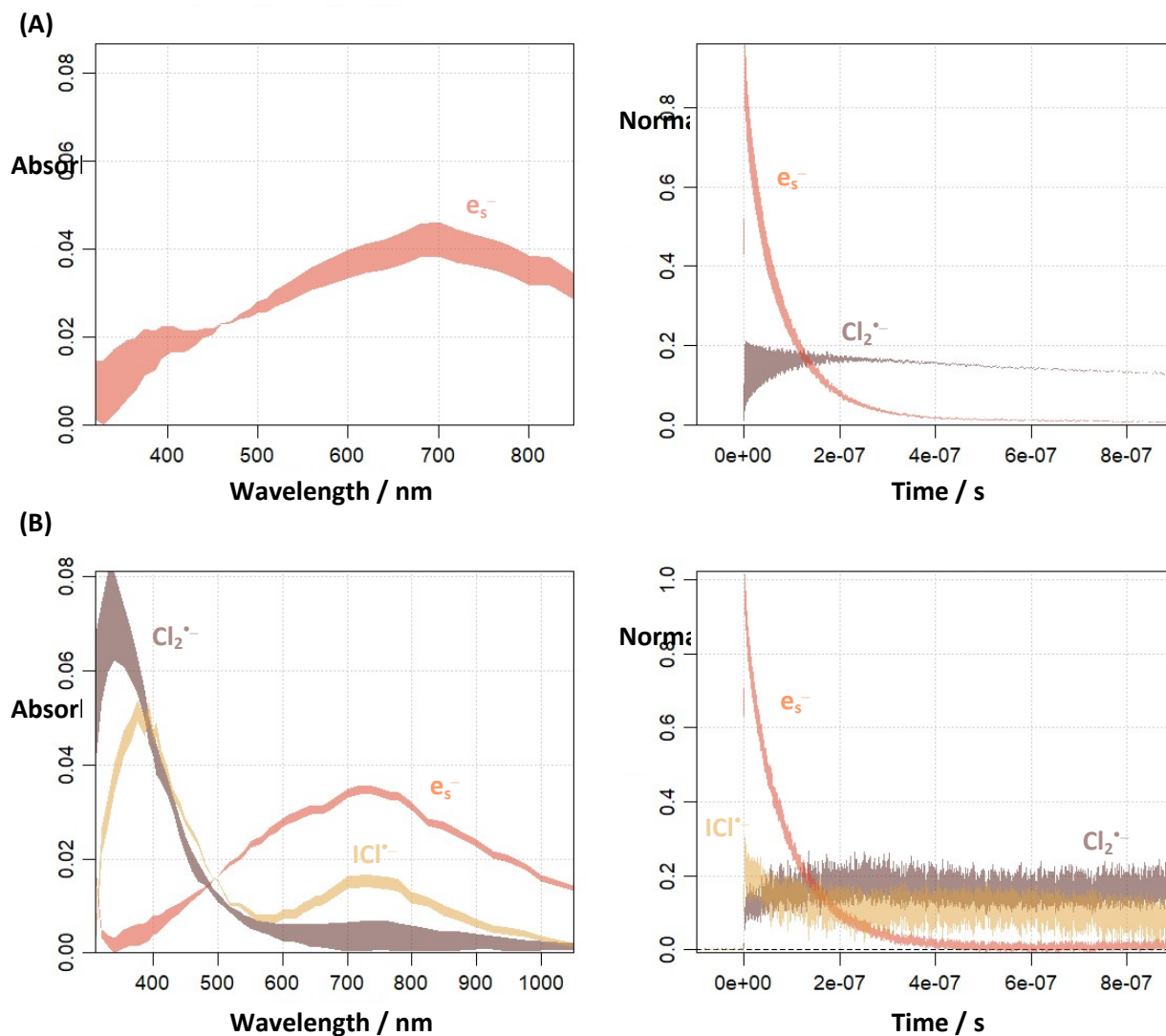


Fig. S2. Ambiguity plots for the kinetics and spectral shapes displayed with equal areas from *SK-Ana* deconvolution of the electron pulse irradiation of neat LiCl-KCl eutectic (A) and 10 wt.% KI in LiCl-KCl eutectic (B) at 400 °C up to 1 μ s. These correspond to the best fit plots given in Fig. 2 in the manuscript.

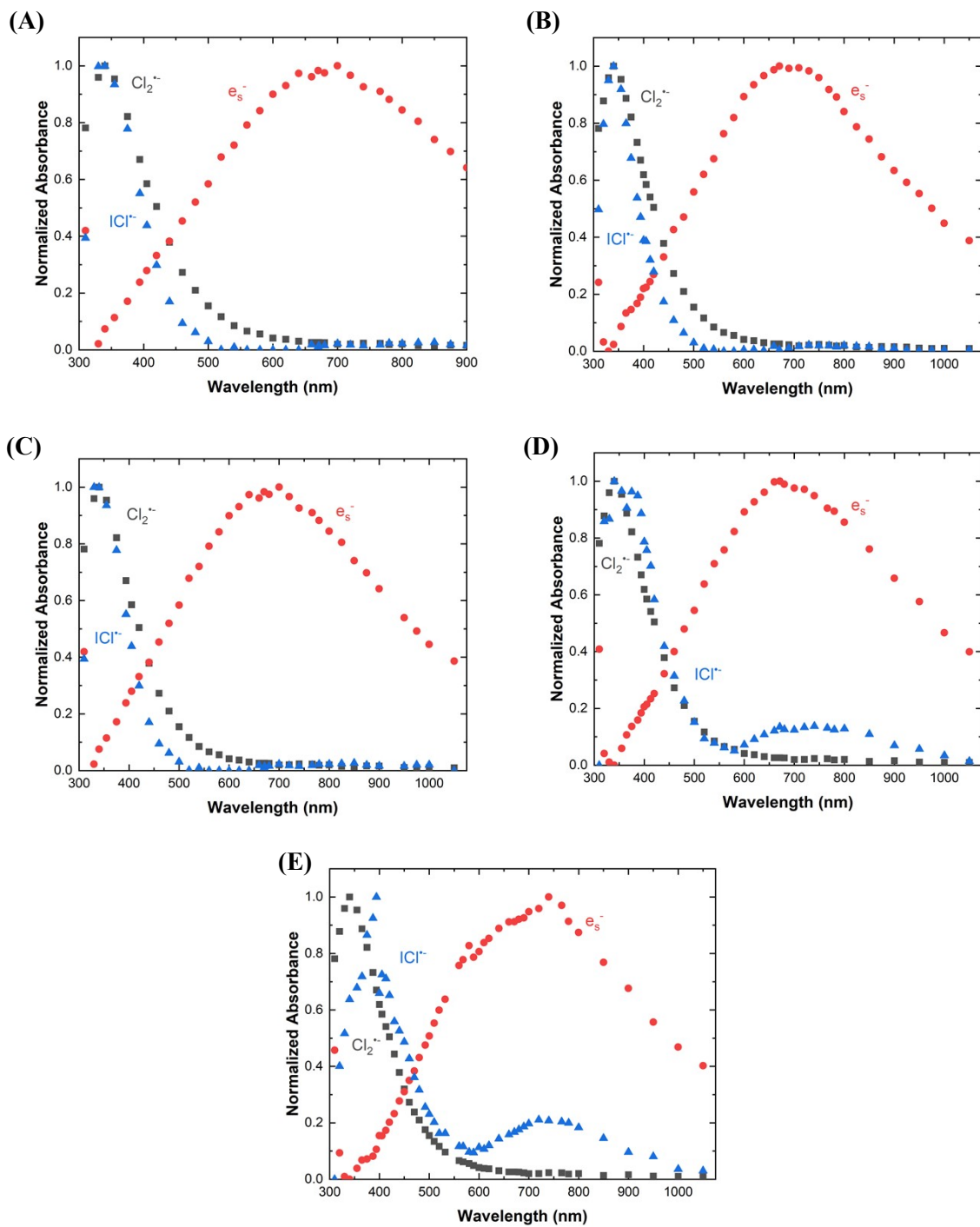


Fig. S3. Normalized spectra from *SK-Ana* deconvolution of the electron pulse irradiation of 0.054 (A), 0.107 (B), 0.536 (C), 1.072 (D), and 5.107 (E) wt.% KI in LiCl-KCl eutectic at 400 °C up to 1 μ s.

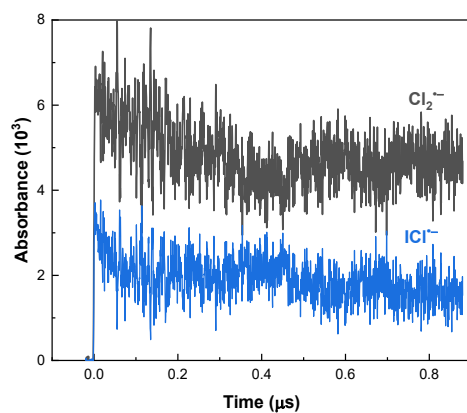


Fig. S4. Deconvoluted kinetic traces after electron pulse irradiation of 10 wt.% KI in LiCl-KCl eutectic with 2 wt.% ZnCl₂ at 400 °C.

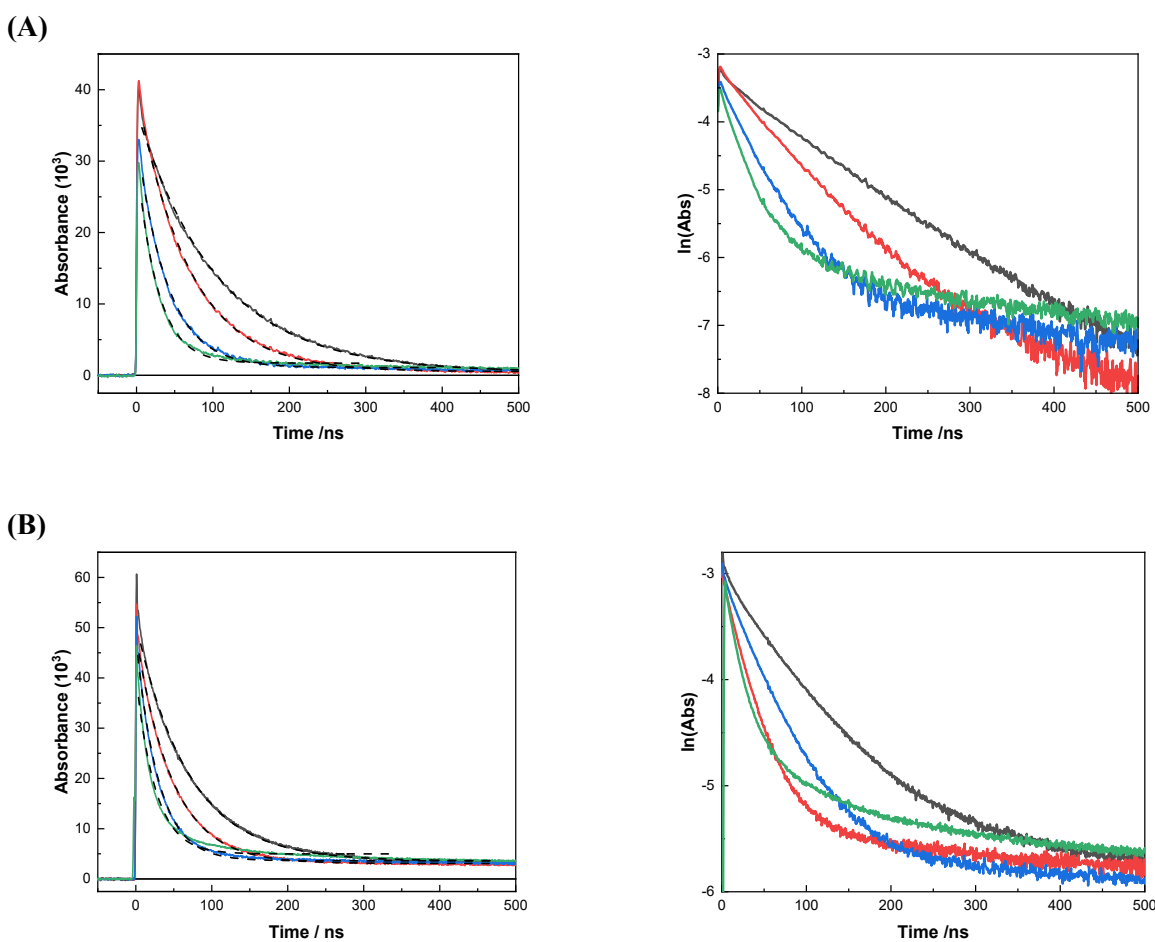


Fig. S5. Dose corrected absorbances at 671 nm and the natural logarithm of those absorbances as a function of time from 0–500 ns demonstrating the decay of the e_s⁻ after the electron pulse irradiation of (A) LiCl-KCl eutectic and (B) 9.998 wt.% KI in LiCl-KCl eutectic at 400 (—), 500 (—), 600 (—), and 700 (—) °C.

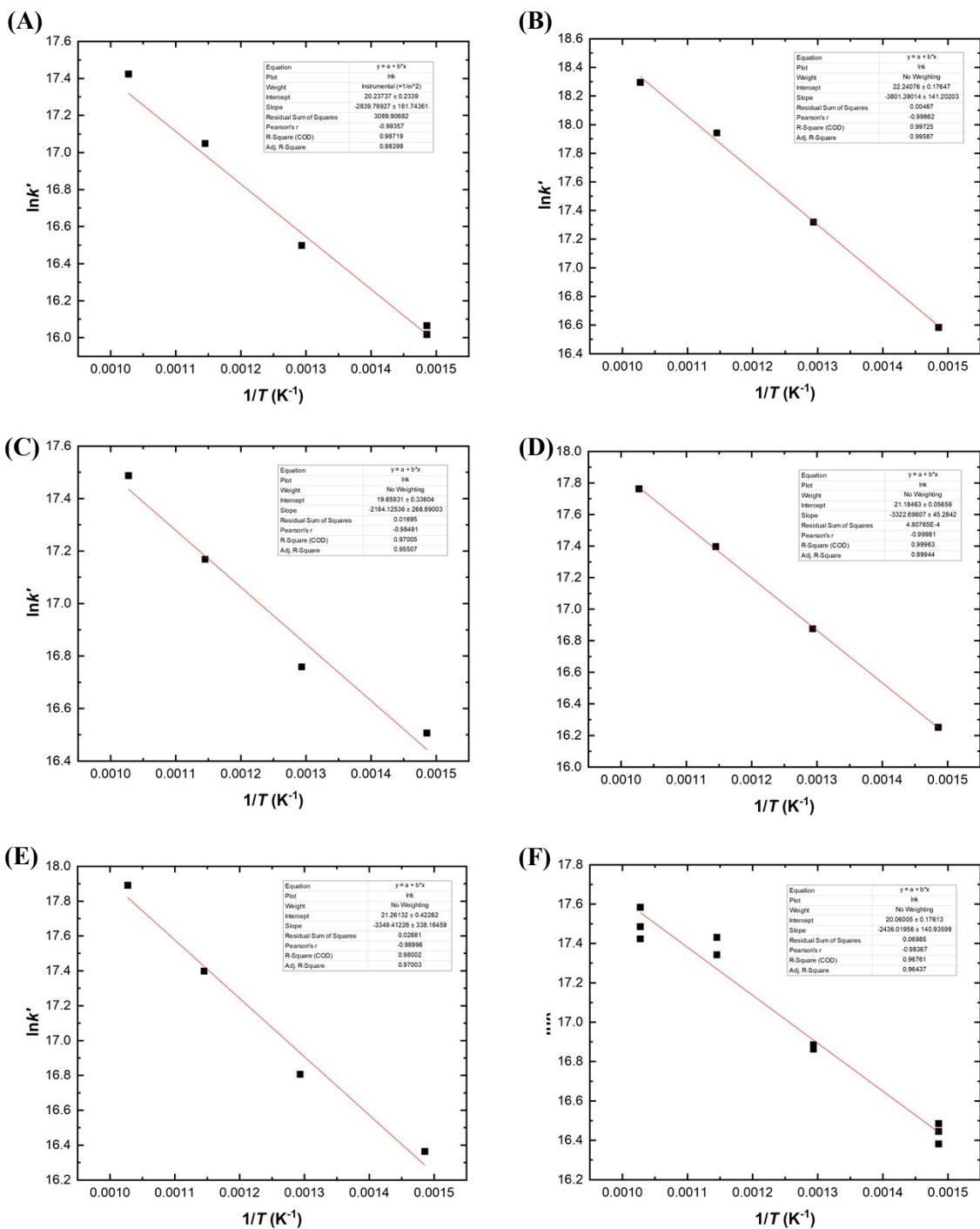


Fig. S6. Plot of the natural logarithm of the pseudo-first-order fits to solvated electron decay vs. the inverse temperature for 0.000 (A), 0.107 (B), 0.536 (C), 1.072 (D), 5.107 (E), and 9.998 (F) wt.% KI in LiCl-KCl molten eutectic.

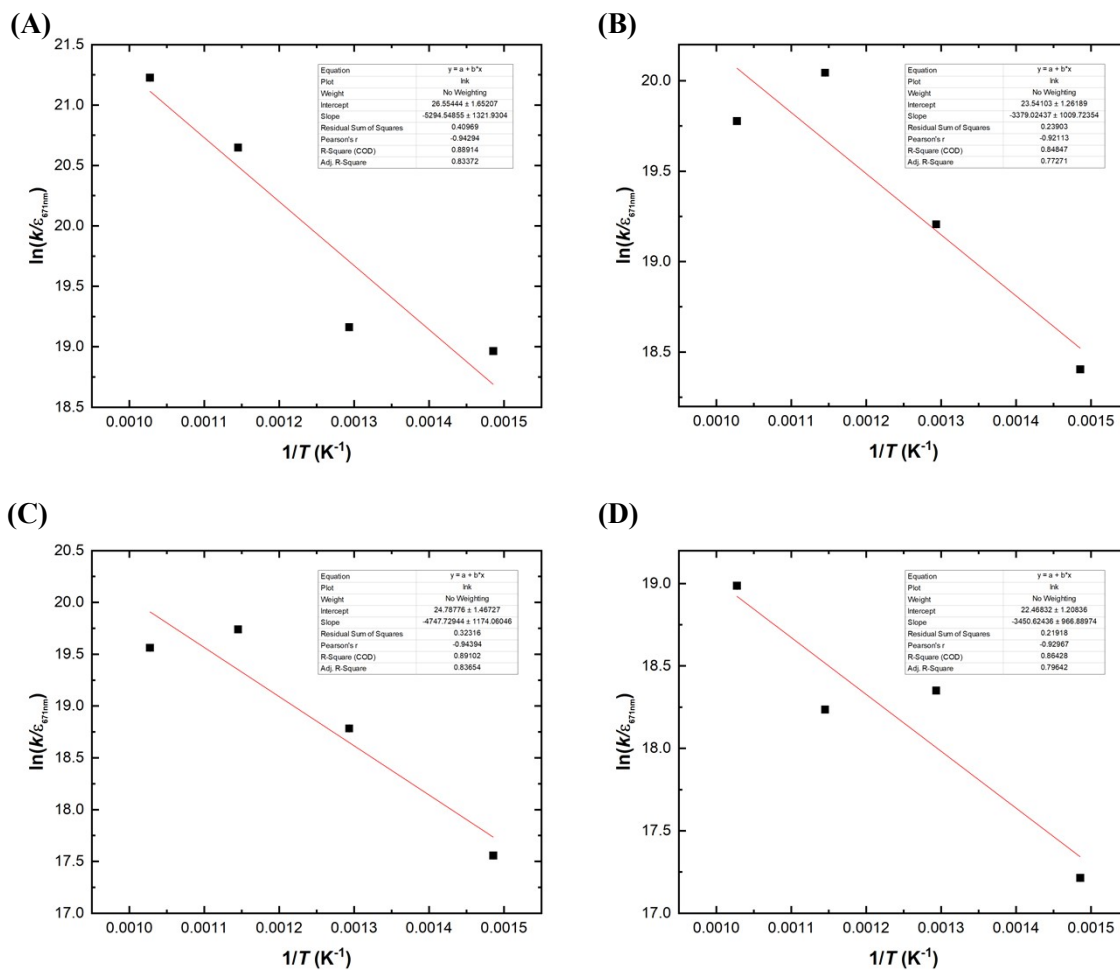


Fig. S7. Plot of the natural logarithm of the fitted k/ϵ_{671nm} for the ICl^- radical cation decay vs. the inverse temperature for 0.107 (A), 0.536 (B), 1.072 (C), and 5.107 (D) wt.% KI in LiCl-KCl molten eutectic.

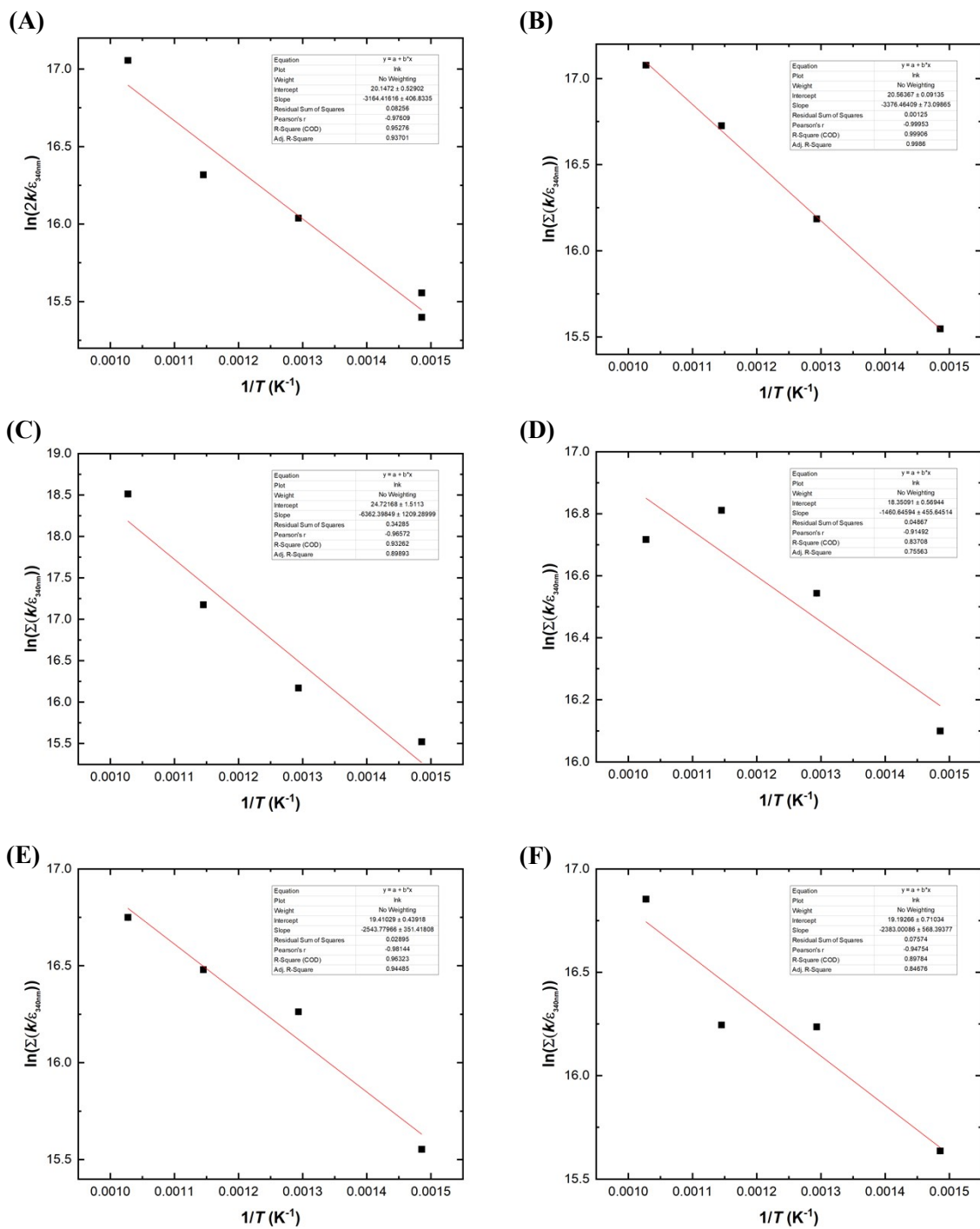


Fig. S8. Arrhenius plots for the overall second-order fits of the combined Cl_2^- and ICl^- radical decay vs. the inverse temperature for 0.000 (A), 0.054 (B), 0.107 (C), 0.536 (D), 1.072 (E), and 5.107 (F) wt.% KI in LiCl-KCl eutectic at 340 nm.

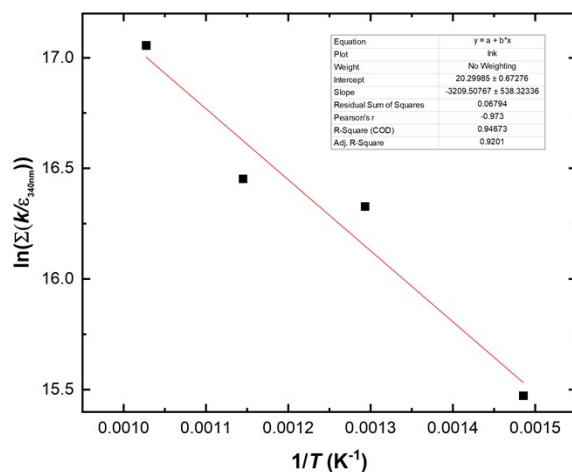


Fig. S9. Arrhenius plots for the overall second-order fits of the combined $\text{Cl}_2^{\cdot-}$ and $\text{ICl}^{\cdot-}$ radical decay vs the inverse temperature for 5.107 wt.% KI in LiCl-KCl eutectic at 400 nm.

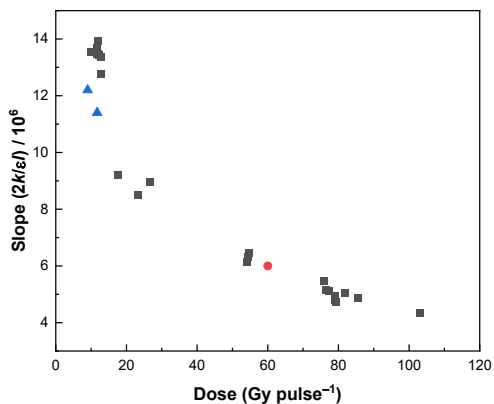


Fig. S10. $\text{Cl}_2^{\cdot-}$ radical anion decay rate ($2k/\epsilon t$) vs. the dose per pulse after the electron pulse irradiation of neat LiCl-KCl eutectic from: this work (\square), Iwamatsu *et al.* (\blacksquare), and Hagiwara *et al.* (\bullet).

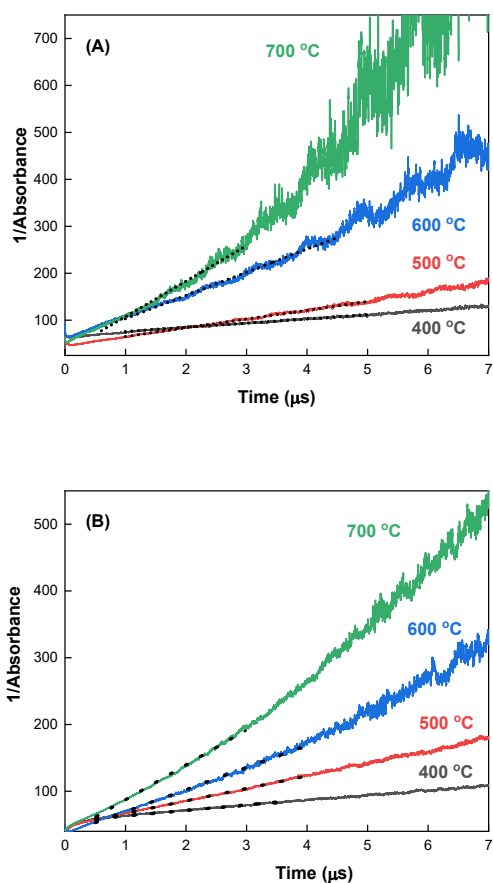


Fig. S11. The fitted inverse absorbance at 340 nm (A) and 400 nm (B) after the electron pulse irradiation of 10 wt.% KI in LiCl-KCl eutectic at 400 (—), 500 (—), 600 (—), and 700 (—) °C.

Table S1. Fitted pseudo-first-order rate coefficients for the decay of the solvated electron at 671 nm.

[KI] (wt.%)	Pseudo-first-order rate coefficients for the e_s^- decay at 671 nm ($k^{\prime} / 10^7 \text{ s}^{-1}$)			
	400 °C	500 °C	600 °C	700 °C
0.000	0.909 ± 0.001	1.462 ± 0.002	2.536 ± 0.007	3.69 ± 0.02
0.054	1.287 ± 0.003	2.518 ± 0.006	4.30 ± 0.02	6.08 ± 0.07
0.107	1.591 ± 0.003	3.32 ± 0.01	6.20 ± 0.03	8.8 ± 0.1
0.536	1.474 ± 0.003	1.898 ± 0.004	2.859 ± 0.009	3.93 ± 0.03
1.072	1.142 ± 0.002	2.134 ± 0.004	3.59 ± 0.01	5.18 ± 0.05
5.107	1.278 ± 0.003	1.992 ± 0.005	3.60 ± 0.01	5.89 ± 0.05
9.998	1.097 ± 0.002	2.111 ± 0.006	3.71 ± 0.02	5.35 ± 0.06